The Journal of Physical Chemistry B

 VOLUME 103, NUMBER 40, OCTOBER 7, 1999

LETTERS

Load-Independent Friction: MoO_3 Nanocrystal Lubricants

Jianfang Wang, Kai C. Rose, and Charles M. Lieber*

Department of Chemistry and Chemical Biology, 12 Oxford Street, Harvard University, Cambridge, Massachusetts 02138

Received: June 23, 1999; In Final Form: August 5, 1999

The behavior of the model lubricant system molybdenum disulfide (MoS_2) has been characterized as a function of thermal oxidation on the atomic to nanometer scales with scanning tunneling microscopy (STM) and atomic force microscopy (AFM) in ultrahigh vacuum (UHV). STM studies of single-crystal MoS_2 surfaces showed that the initial stages of thermal oxidation produce atomic-scale pits and then molybdenum oxide (MoO_3) nanocrystals 1−5 nm in diameter. The densities of pits and MoO_3 nanocrystals and the size of MoO_3 nanocrystals increased with increasing oxidation time. UHV AFM friction measurements made on these same samples exhibited a direct relationship between defect density and friction for short oxidation times. After longer oxidation times when well-defined MoO_3 nanocrystals were present, load-independent friction was observed. A model, which involves adhesion of MoO_3 nanocrystals to the AFM probe tip end, has been developed to explain this first observation of load-independent friction. The implications of these results are discussed.

Introduction

Macroscopic studies of friction, adhesion, and wear have contributed much to the phenomenological understanding of tribology.[1−3] However, studies of the interactions between macroscopic bodies are influenced by complex factors, including surface roughness and adsorbates, that make it difficult to develop a fundamental atomistic understanding of friction.[2−4] Nanometer-scale measurements of friction and intermolecular forces can disentangle the complex factors contributing to friction, and thus provide data needed for developing microscopic models and designing improved lubricants rationally.[2−5] Such microscopic information is also of importance to many areas of nanoscale science and technology, including manipulation and assembly of nanostructures and understanding the behavior of microelectromechanical systems (MEMS).[3−5]

AFM can be used to measure normal and lateral forces on the nanometer scale, and thus represents a powerful tool for probing the microscopic mechanisms of friction.[4−13] Studies of friction between probe tips and different surfaces have yielded a number of interesting observations, including atomic scale stick−slip motion,[6,7] a linear dependence of friction force on contact area,[8−11,13] functional-group dependence of friction,[11,12] and friction anisotropy.[7,13] Many of these studies have been carried out on atomically flat surfaces where the defect density is expected to be small, although this density typically has not been characterized and correlated with friction. On the macroscopic scale, however, defects exist at solid−solid sliding interfaces. Because it is possible that defects dominate energy dissipation during sliding, it is essential to determine explicitly their contribution to the observed friction between moving bodies.

To address how surface defects influence friction, we have systematically characterized thermally generated defects on surfaces of the model solid lubricant MoS_2 using UHV STM and determined the resulting changes in friction on the same samples by UHV AFM. First, UHV STM measurements on single-crystal MoS_2 surfaces show that thermal oxidation

* Author to whom correspondence should be addressed. E-mail: cml@cmliris.harvard.edu.

10.1021/jp9920794 CCC: $18.00
Published on Web 09/15/1999

produces atomic-scale pits and subsequently MoO_3 nanocrystals 1−5 nm in diameter. The densities of pits and MoO_3 nanocrystals, and the size of MoO_3 nanocrystals increase with increasing oxidation time. Subsequent UHV AFM friction measurements on the same oxidized single-crystal MoS_2 surfaces show that initially, frictional forces increase with increasing number density of defects. However, when well-defined nanometer-scale MoO_3 crystallites are produced at longer oxidation times, load-independent friction is observed. These results suggest that nanometer-scale materials can be utilized to design lubricants with improved performance.

Experimental Section

The growth and characterization of MoO_3 nanocrystals on single-crystal MoS_2 surfaces have been described previously.[13,14] In our experiments, freshly cleaved, single-crystal 2H−MoS_2 surfaces were oxidized in purified oxygen at 470 °C for several minutes. After oxidation, these samples, together with a freshly cleaved, unoxidized MoS_2 sample, were transferred into a UHV chamber (base pressure $< 5 \times 10^{-10}$ Torr) equipped with a commercial AFM/STM (Omicron). UHV AFM and STM investigations were carried out at room temperature. STM imaging studies were made using electrochemically etched tungsten tips in the constant current mode with the bias voltage applied to the sample. AFM friction measurements were made with bare, Au-coated (5 nm Cr adhesion promoter; 50 nm Au) and Ti-coated (16 nm Ti) Si_3N_4 tips. The modified Si_3N_4 tips were coated in an electron-beam evaporator. Friction measurements were taken on atomically flat single-crystal MoS_2 terraces. The maximum applied loads were about 30 nN below that at which wear was observed. All friction measurements were performed with a sliding velocity of 5 μm/s. Data points on friction-versus-load plots were obtained by taking both forward and reverse friction images with an image size of 1×1 μm and a resolution of 512×512 pixels. To determine the friction value from the forward and reverse images, first the friction value for every single line was calculated as half of the average of the difference between the reverse and corresponding forward friction scan lines. Then, a histogram, containing 512 line friction values, was used to determine the average friction force using a Gaussian fit. Normal cantilever force constants were obtained from the cantilever thermal noise spectrum.[15] Friction forces were calibrated using a stepped (305) surface of a $SrTiO_3$ crystal.[16]

Results and Discussion

Typical STM images of freshly cleaved and thermally oxidized MoS_2 single-crystal surfaces are shown in Figure 1. Nanometer-scale circular features (4−5 nm in diameter), which appear dark at both negative and positive sample bias voltages, are observed on the freshly cleaved surfaces (Figure 1a). Previous studies have attributed these features to acceptor metal impurities substituted for Mo atoms.[17] The fact that the observed density of these defects is similar to the concentration of known metal impurities (Ti and V) in the natural single-crystal MoS_2 samples used in our experiments,[18] and that the density is approximately constant for unoxidized and oxidized MoS_2 surfaces (Table 1) is consistent with this previous assignment. Thermal oxidation at 470 °C produces two new types of defects: atomic-scale surface pits and larger raised structures 1−5 nm in diameter (Figure 1, parts b and c, respectively). The average number densities of both of these new defects obtained from about 30 STM images on each type of sample, increase with increasing oxidation time (Table 1). Cross sections recorded

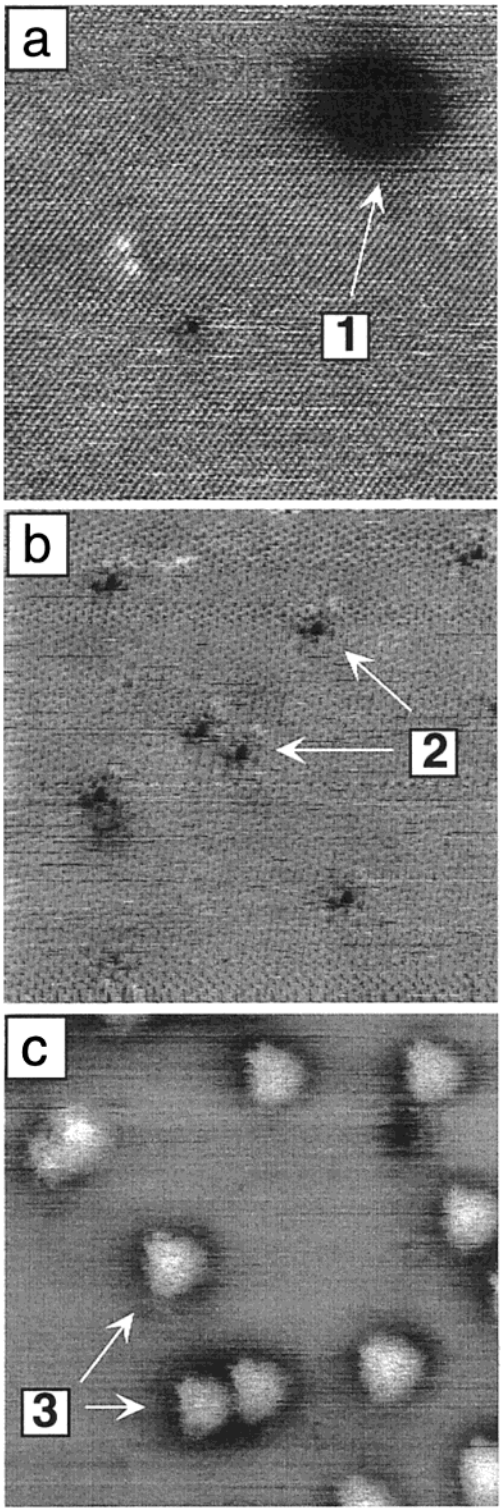

Figure 1. Typical STM images of (a) a freshly cleaved MoS_2 surface, obtained with a sample bias voltage $V_{bias} = +0.6$ V and a tunnel current $I = 0.1$ nA, (b) MoS_2 surface oxidized at 470 °C for 5 min, obtained with $V_{bias} = -0.6$ V and $I = 0.2$ nA, (c) MoS_2 surface oxidized at 470 °C for 7 min, obtained with $V_{bias} = -0.7$ V and $I = 0.1$ nA. Surface structures labeled 1, 2, 3 are metal impurities, atomic-scale surface pits, and MoO_3 nanocrystals, respectively (see text for explanation). Image sizes are 20 nm by 20 nm.

across the pits show depths, 0.6−0.7 nm, consistent with removal of material from a single S−Mo−S layer. The raised 1−5 nm structures, which can be moved by the STM tip during scanning, have heights of 0.5−0.9 nm. Previous X-ray photoemission studies have shown that MoO_3 can be detected after

TABLE 1: Defect Densities on MoS_2 Surfaces

	defect types (10^{10}/cm^2)		
sample	substitutional impurities	atomic pits	MoO_3 nanocrystals
freshly cleaved	5 ± 3	0	0
5 min oxidized	4 ± 2	50 ± 10	11 ± 8
7 min oxidized	3 ± 1	510 ± 90	190 ± 80

oxidation at 460 °C for 5 min in purified oxygen.[14] Moreover, we have shown previously that more extensive oxidation (480 °C, 5−10 min) produces MoO_3 nanocrystals 1−3 unit cells thick and 200−500 nm on edge, and that these nanocrystals can be manipulated with the AFM tip.[13,14] Taken together, these results strongly suggest that the 1−5 nm diameter structures observed in our experiments are MoO_3 nanocrystals.

To investigate how these defects affect friction, we have used AFM to characterize friction in UHV. The same samples characterized by STM were investigated without removing them from the UHV environment. Figure 2a shows that the friction force on a partially oxidized MoS_2 surface (470 °C for 5 min) is 2−3 times larger than that on a freshly cleaved MoS_2 surface for similar applied loads with the same tip. The friction force shows an almost linear load dependence on these two MoS_2 surfaces with the friction coefficient on the slightly oxidized MoS_2 surface 1.5 times larger than that on the freshly cleaved MoS_2 surface. On the basis of these data and the STM results, we conclude that the friction force and friction coefficient increase with increasing number density of surface defects. The tip−surface contact area estimated from the Hertz model is 10−30 nm^2 within the range of loads applied in the experiments. Taking into account the number density of surface defects (Table 1), there are at most two defects under the tip at any time. The increase of friction can thus be associated with interactions at these defect sites. The dangling bonds at surface pits should increase the shear stress between the tip and MoS_2 surfaces. Although we did not observe spatial variations in friction in these experiments, we expect that such variations should be observable with smaller tips. The fact that these surface defects cannot be observed with AFM, due to the finite size of the probe tip, highlights the importance of structural characterization down to the atomic scale in nanotribology.

The number densities of surface pits and MoO_3 nanocrystals on the oxidized MoS_2 surfaces increase further with oxidation time (7 min samples), thus suggesting that friction should increase as well. Figure 2a shows that this is indeed true for small applied loads. However, a completely different behavior—load-independent friction—is observed at higher loads. To the best of our knowledge, this is the first time that load-independent friction has been observed. We have carried out a number of studies to investigate the reproducibility and origin of this remarkable observation. First, the same tip was used to measure friction forces vs load at different positions on the 7 min oxidized MoS_2 surface. Almost all of the measurements were found to exhibit load-independent friction. Five typical friction-versus-load plots are shown in Figure 2b. To ensure that our observation of load-independent friction was not related to the use of a particular tip, we also measured friction forces on 7 min oxidized MoS_2 surfaces with other uncoated, Au-coated and Ti-coated Si_3N_4 tips. When using a clean tip for the first time, often a linear increase in friction at lower loads followed by a sudden drop to a constant friction value at higher loads is found. A representative plot obtained with an uncoated new Si_3N_4 tip is shown in Figure 2c. Subsequent measurements made with these tips showed load-independent friction in more than 80% of the experiments. Shown in Figure 2d are three representative plots obtained with a Si_3N_4 tip, a Au-coated Si_3N_4 tip, and a Ti-coated Si_3N_4 tip. These latter data also show that specific tip chemistry does not give rise to the load-independent

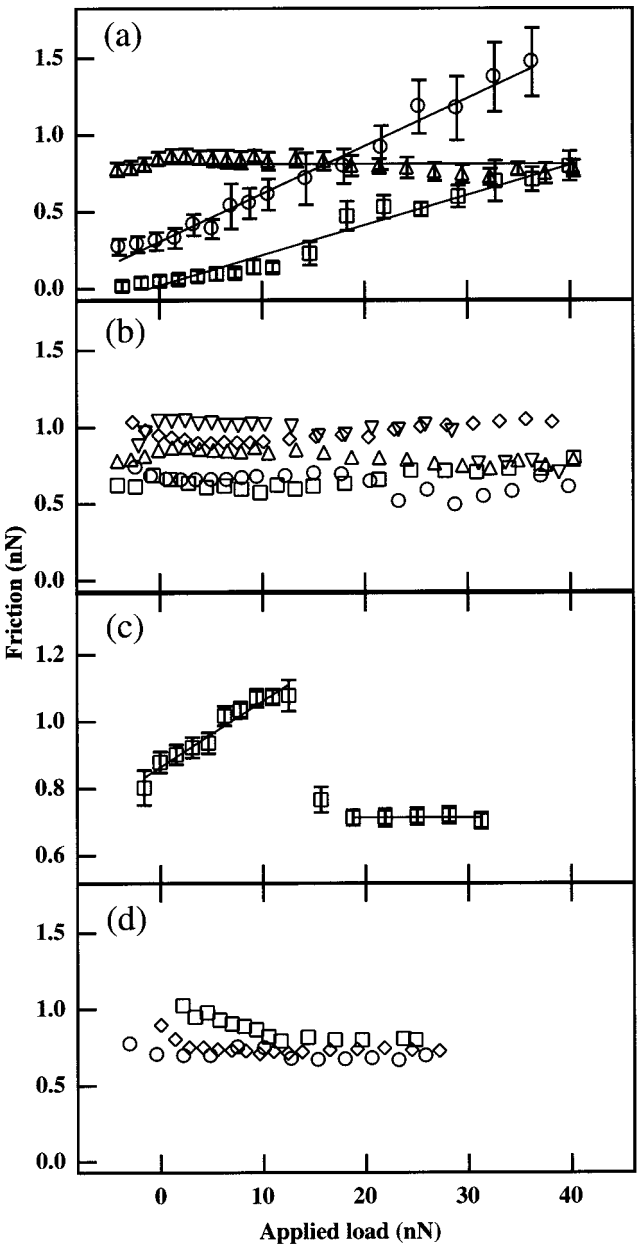

Figure 2. (a) Typical plots of friction versus applied load obtained with a bare Si_3N_4 tip on freshly cleaved (squares), 5 min oxidized (circles), and 7 min oxidized (triangles) MoS_2 surfaces. The friction coefficients on the freshly cleaved and 5 min oxidized MoS_2 surfaces are 0.020 ± 0.001 and 0.031 ± 0.001, respectively. The solid lines on the plots for the freshly cleaved and 5 min oxidized MoS_2 surfaces are linear least-squares fits to the data. The solid line on the plot for the 7 min oxidized MoS_2 surface is an average of all friction values. The adhesion forces determined from force−distance curves are 9 ± 1, 7.0 ± 0.6, and 8.3 ± 0.5 nN (in the order of squares, circles, and triangles). They are the same within the range of error on the three MoS_2 surfaces. (b) Friction vs load data obtained with the same Si_3N_4 tip as in (a) at different positions on a MoS_2 surface oxidized for 7 min. (c) Friction vs load results for a new Si_3N_4 tip on a 7 min oxidized MoS_2 surface. Similar behavior was also observed using new Au-coated and Ti-coated tips. The friction coefficient of the linear part, 0.020 ± 0.002, is smaller than that on the 5 min oxidized MoS_2 surface because a different tip was used here (tip radius: 28 nm). (d) Friction vs load data obtained on a 7 min oxidized MoS_2 surface with an uncoated Si_3N_4 tip (circles), a Au-coated Si_3N_4 tip (squares), and a Ti-coated Si_3N_4 tip (diamonds). The uncoated Si_3N_4 tip used in (d) is the same one as in (c). The error bars in (b) and (d) are similar to those in (a).

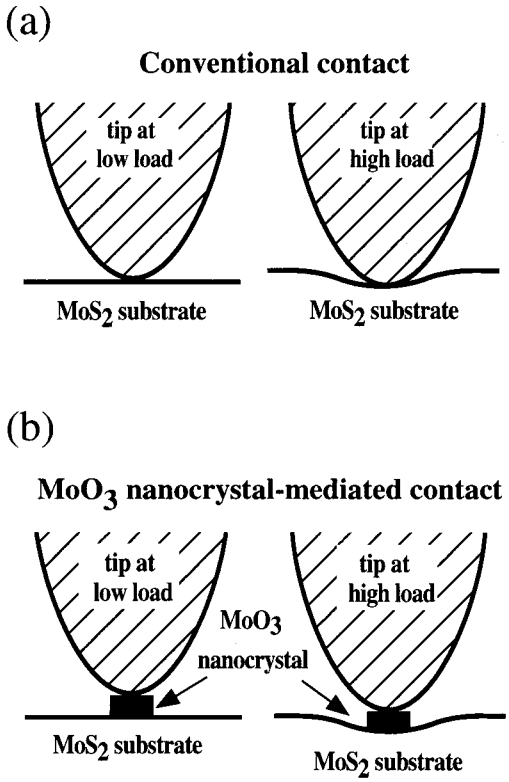

Figure 3. Models of conventional and MoO_3 nanocrystal-mediated tip−surface contact. See text for explanation.

friction, and thus suggests that it is due to a property of the oxidized MoS_2 surface.

To explain the observed load-independent friction behavior, we propose a model in which the tip−surface contact is mediated by a MoO_3 nanocrystal (Figure 3). When a probe tip is scanning on the oxidized MoS_2 surface, a MoO_3 nanocrystal can adhere to the apex of the tip. This produces a spacer between the tip and substrate whereby the contact interface area is defined by the nanocrystal size, and the contact area does not change with load. Such a fixed-area sliding contact can explain the observed load-independent friction. This model is also in agreement with the fact that when tips are used for the first time, friction increases linearly at low loads and suddenly drops to a constant friction value at higher loads; that is, the drop occurs when a MoO_3 nanocrystal becomes fixed between the tip and substrate.[19]

In contrast, the contact area in a conventional contact between a tip and a surface increases with load, and thus friction increases with load as shown in Figure 3a. We did not observe load-independent friction on the MoS_2 surface oxidized at 470 °C for 5 min. This suggests that there exists a critical size of MoO_3 nanocrystals needed to enable this phenomena. Although the average size increased only slightly with oxidation time, some MoO_3 nanocrystals were observed to grow together to form larger nanocrystals (5 nm by 3 nm) on the MoS_2 surface oxidized at 470 °C for 7 min. For MoO_3 nanocrystals with observed sizes ranging from 1 to 5 nm in diameter, the contact pressure is estimated to range from 50 to 2 GPa at the maximum applied load of 40 nN in our experiments. For the most common 2 nm nanocrystal size, the contact pressure is 13 GPa. These pressures are higher than the typical values, 0.1−2GPa, obtained in studies where single-asperity probe tips have been used and the load dependence of the contact area has been described using continuum mechanics models.[8−10] In addition, we estimate that the shear stress between MoO_3 nanocrystals and MoS_2 substrate ranges from 950 to 40 MPa for 1−5 nm MoO_3 nanocrystals with a value of 240 MPa for the typical 2 nm nanocrystal size.[20] The shear stress determined from macroscopic friction measurements on MoS_2 thin films ranges from 20 to 80 MPa in different gaseous environments.[21] In our experiments, the exact area of the MoO_3 nanocrystal adhering to the tip end is unknown. If we consider larger (5 nm) MoO_3 nanocrystals, the estimated shear stress, 40 MPa, is of the same order as macroscopic values.

Few studies have investigated the sliding of well-defined nanostructures.[13,22,23] These include lattice-directed sliding of larger MoO_3 nanocrystals on MoS_2,[13] sliding of C_{60} islands on single-crystal NaCl(001),[22] and rolling and sliding of carbon nanotubes on sufaces.[23] The forces to slide or roll these nanostructures have been measured, and have enabled well-defined shear stresses to be determined. But the load dependence of these forces has not been studied. Recent studies on spherical nanoparticles have shown that rolling rather than sliding of these nanoparticles might play an important role in their performance as lubricants.[24,25] These nanoparticles include C_{60} clusters[24] and related hollow WS_2 cage structures.[25] Our results reported here indicate that MoO_3 nanocrystals with a layered structure can adhere to one sliding interface as a spacer. The MoO_3 nanocrystals then maintain a constant sliding contact area under different loads, and produce load-independent friction.[26] We believe that this idea represents a potential approach for designing new lubricants for macroscopic contacts, and for nano- and microelectromechanical systems.

Acknowledgment. This work was supported by the Air Force Office of Scientific Research (F49620-94-1-0010). K.C.R. is grateful to the support from the German Academic Exchange Service (DAAD/HSP III-Program).

References and Notes

(1) Bowden, F. P.; Tabor, D. *The Friction and Lubrication of Solids*; Clarendon: Oxford, 1964; Part II.

(2) *Fundamentals of Friction: Macroscopic and Microscopic Processes*; Singer, I. L., Pollock, H. M., Eds.; Kluwer: Dordrecht, 1992.

(3) *Handbook of Micro/Nanotribology*; Bhushan, B., Ed.; CRC Press: Boca Raton, FL, 1995. *Tribology Issues and Opportunities in MEMS*; Bhushan, B., Ed.; Kluwer: Boston, 1998.

(4) Singer, I. L. *J. Vac. Sci. Technol. A* **1994**, *12*, 2605. Bhushan, B.; Israelachvili, J. N.; Landman, U. *Nature* **1995**, *374*, 607. Krim, J. *Sci. Am.* **1996**, *275*, 74. Rozman, M. G.; Urbakh, M.; Klafter, J.; Elmer, F.-J. *J. Phys. Chem. B* **1998**, *102*, 7924. Harrison, J. A.; Perry, S. S. *MRS Bulletin* **1998**, *23*, 27. Landman, U. *Solid State Commun.* **1998**, *107*, 693.

(5) Mate, C. M. *IBM J. Res. Dev.* **1995**, *39*, 617. Carpick, R. W.; Salmeron, M. *Chem. Rev.* **1997**, *97*, 1163.

(6) Mate, C. M.; McClelland, G. M.; Erlandsson, R.; Chiang, S. *Phys. Rev. Lett.* **1987**, *59*, 1942.

(7) Overney, R. M.; Takano, H.; Fujihira, M.; Paulus, W.; Ringsdorf, H. *Phys. Rev. Lett.* **1994**, *72*, 3546.

(8) Carpick, R. W.; Agraït, N.; Ogletree, D. F.; Salmeron, M. *J. Vac. Sci. Technol. B* **1996**, *14*, 1289. Carpick, R. W.; Agraït, N.; Ogletree, D. F.; Salmeron, M. *Langmuir* **1996**, *12*, 3334. Meyer, E.; Lüthi, R.; Howald, L.; Bammerlin, M.; Guggisberg, M.; Güntherodt, H.-J. *J. Vac. Sci. Technol. B* **1996**, *14*, 1285.

(9) Lantz, M. A.; O'Shea, S. J.; Welland, M. E.; Johnson, K. L. *Phys. Rev. B* **1997**, *55*, 10776. Enachescu, M.; van den Oetelaar, R. J. A.; Carpick, R. W.; Ogletree, D. F.; Flipse, C. F. J.; Salmeron, M. *Phys. Rev. Lett.* **1998**, *81*, 1877.

(10) Schwarz, U. D.; Zwörner, O.; Köster, P.; Wiesendanger, R. *Phys. Rev. B* **1997**, *56*, 6987; and *Phys. Rev. B* **1997**, *56*, 6997. Schwarz, U. D.; Allers, W.; Gensterblum, G.; Wiesendanger, R. *Phys. Rev. B* **1995**, *52*, 14976.

(11) Frisbie, C. D.; Rozsnyai, L. F.; Noy, A.; Wrighton, M. S.; Lieber, C. M. *Science* **1994**, *265*, 2071. Noy, A.; Frisbie, C. D.; Rozsnyai, L. F.; Wrighton, M. S.; Lieber, C. M. *J. Am. Chem. Soc.* **1995**, *117*, 7943. Vezenov, D. V.; Noy, A.; Rozsnyai, L. F.; Lieber, C. M. *J. Am. Chem. Soc.* **1997**, *119*, 2006.

(12) Overney, R. M.; Meyer, E.; Frommer, J.; Güntherodt, H.-J.; Fujihira, M.; Takano, H.; Gotoh, Y. *Langmuir* **1994**, *10*, 1281. Green, J. B. D.; McDermott, M. T.; Porter, M. D.; Siperko, L. M. *J. Phys. Chem.* **1995**, *99*, 10960. Marti, A.; Hahner, G.; Spencer, N. D. *Langmuir* **1995**, *11*, 4632.

Sinniah, S. K.; Steel, A. B.; Miller, C. J.; Reutt-Robey, J. E. *J. Am. Chem. Soc.* **1996**, *118*, 8925. Kim, H. I.; Koini, T.; Lee, T. R.; Perry, S. S. *Langmuir* **1997**, *13*, 7192. Burns, A. R.; Houston, J. E.; Carpick, R. W.; Michalske, T. A. *Phys. Rev. Lett.* **1999**, *82*, 1181.

(13) Sheehan, P. E.; Lieber, C. M. *Science* **1996**, *272*, 1158.

(14) Kim, Y.; Lieber, C. M. *Science* **1992**, *257*, 375. Kim, Y. Ph.D. Thesis, Harvard University, Cambridge, MA, 1992.

(15) Hutter, J. L.; Bechhoefer, J. *Rev. Sci. Instrum.* **1993**, *64*, 1868.

(16) Ogletree, D. F.; Carpick, R. W.; Salmeron, M. *Rev. Sci. Instrum.* **1996**, *67*, 3298.

(17) Whangbo, M.-H.; Ren, J.; Magonov, S. N.; Bengel, H.; Parkinson, B. A.; Suna, A. *Surf. Sci.* **1995**, *326*, 311.

(18) Ha, J. S.; Roh, H.-S.; Park, S.-J.; Yi, J.-Y.; Lee, E.-H. *Surf. Sci.* **1994**, *315*, 62.

(19) After the initial transition to load-independent friction with a new tip, subsequent measurements showed load-independent friction in over 80% of our experiments. In the remaining measurements (<20%), these tips did not exhibit load-independent behavior nor did they exhibit friction linearly dependent on load. We believe that these latter cases likely reflect the removal or addition of MoO_3 nanocrystals during scanning.

(20) The variation in MoO_3 nanocrystal size should also lead to a variation in the observed load-independent friction forces; that is, different nanocrystal areas will produce different constant friction values. The observed variation in load-independent friction (i.e., Figure 2, parts b and d, could arise from such variations. However, for a constant shear stress we would expect a greater variation of constant friction force (based on the 1−5 nm variation in nanocrystal size). Future transmission electron microscopy imaging studies of tips exhibiting load-independent friction should provide insight into this issue.

(21) Singer, I. L.; Bolster, R. N.; Wegand, J.; Fayeulle, S.; Stupp, B. C. *Appl. Phys. Lett.* **1990**, *57*, 995. Grosseau-Poussard, J. L.; Moine, P.; Brendle, M. *Thin Solid Films* **1997**, *307*, 163.

(22) Lüthi, R.; Meyer, E.; Haefke, H.; Howald, L.; Gutmannsbauer, W.; Güntherodt, H.-J. *Science* **1994**, *266*, 1979.

(23) Falvo, M. R.; Taylor, R. M., II; Helser, A.; Chi, V.; Brooks, F. P., Jr.; Washburn, S.; Superfine, R. *Nature* **1999**, *397*, 236. Hertel, T.; Martel, R.; Avouris, P. *J. Phys. Chem. B* **1998**, *102*, 910.

(24) Campbell, S. E.; Luengo, G.; Srdanov, V. I.; Wudl, F.; Israelachvili, J. N. *Nature* **1996**, *382*, 520.

(25) Rapoport, L.; Bilik, Y.; Feldman, Y.; Homyonfer, M.; Cohen, S. R.; Tenne, R. *Nature* **1997**, *387*, 791.

(26) In our previous studies of large MoO_3 nanocrystals,[13] we observed that the friction was highly anisotropic; that is, the nanocrystals could only be moved along specific MoS_2 lattice directions. In the present work, preliminary studies of friction as a function of scan angle provide some evidence for anisotropy (i.e., expected 60° variation), although the effect is not reproducible. It is possible that facile reorientation of the small nanocrystals within the tip−sample contact precludes the observation of friction anisotropy in many cases.